Broadband waveforms and site effects at a borehole seismometer in the Po alluvial basin (Italy)

Massimo Cocco (1), **Fabrizio Ardizzoni** (2), **Riccardo M. Azzara** (1), **Lorella Dall'Olio** (2), **Alberto Delladio** (1), **Massimo Di Bona** (1), **Luca Malagnini** (1), **Lucia Margheriti** (1) **and Anna Nardi** (1)

(1) *Istituto Nazionale di Geofisica e Vulcanologia, Roma, Italy*

(2) *Comune di Ferrara, Italy*

Abstract

Broadband seismograms recorded at a borehole three-component (high dynamic range) seismic station in the Po Valley (Northern Italy) were analyzed to study the velocity structure of the shallow sedimentary layers as well as the local site effects in soft sediments. The broadband borehole seismometer was installed at a depth of 135 m just below the quaternary basement, while a second digital broadband seismometer was installed in the same site at the Earth surface. The velocity structure in the shallower layers was determined both by means of cross-hole and up-hole measurements and by inverting seismic data recorded during a seismic exploration experiment. Velocity discontinuities are quite well related to the stratigraphy of the site. We are interested to record local earthquakes as well as regional and teleseismic events. The analyzed data set includes local, regional and teleseismic events, most of which were recorded during the seismic sequence that started on October 15, 1996, near Reggio Emilia 80 km away from the borehole site. The orientation of the borehole sensor is determined using the recordings of a teleseismic event and of some local earthquakes. The noise reduction for the borehole sensor is 2 decades in power spectral density at frequencies larger than 1.0 Hz. We studied the site amplification of the shallow alluvial layers by applying the spectral ratio method. We analyzed the spectral ratios of noise recorded by the surface and borehole seismometers as well as those from local earthquakes. We compared these observations with a theoretical model for the site response computed by the Haskell-Thomson method.

Key words *broadband data – borehole seismometer – site effects – alluvial basin*

1. Introduction

The detection threshold for local, regional and teleseismic earthquakes of the permanent seismometric stations of the Italian National Telemetered Seismological Network located in the large sedimentary area of the Po Valley (Northern Italy) is significantly higher than that of stations located in the Alps or Apennines. This is due to the unfavorable geological (huge thickness of alluvial layers) and anthropic (proximity of large noise sources) conditions. For this reason and to study the local site response of shallow alluvial layers, we installed a borehole broadband seismometer in the Po plain, near the town of Ferrara and close to the Po River. We also temporarily installed a second broadband seismometer at the surface. Downhole seismometer test sites give the opportunity to improve our understanding of the effects of a shallow soil column on the recorded ground motion at the surface and to test the robustness of the different empirical techniques used in estimat-

Mailing address: Dr. Massimo Cocco, Istituto Nazionale di Geofisica e Vulcanologia, Via di Vigna Murata 605, 00143 Roma, Italy; e-mail: cocco@ingv.it

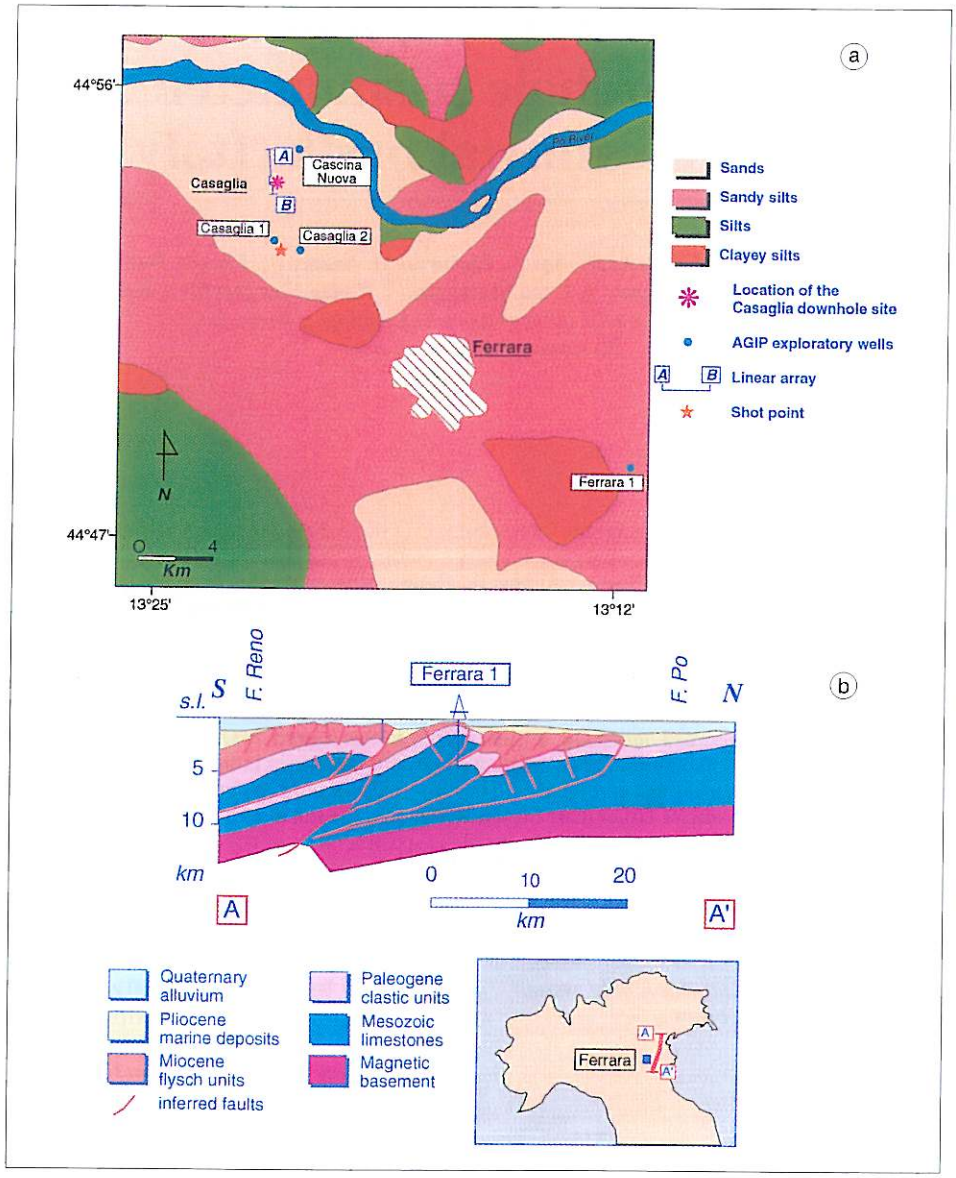

Fig. 1a,b. a) Map view showing the location of the borehole site (indicated by the asterisk), the main geological features outcropping in the area and the position of several exploratory wells (dots) made by the Italian petroleum company (AGIP). The line A-B shows the position of the linear array deployed during the seismic exploration experiment performed to constrain *P*- and *S*-wave velocity in the shallow alluvial layers (the star indicates the shot point). b) The cross-section here reported is part of a nearly NS seismic profile passing very close to the borehole site (see the map in the bottom of the figure and position of the *Ferrara 1* well in the map and in the cross-section). This cross-section points out the Ferrara structural high, where the depth of the quaternary basement is only few hundreds of meters. This is the only place in the Po plain where a 135 m deep well can reach the quaternary basement.

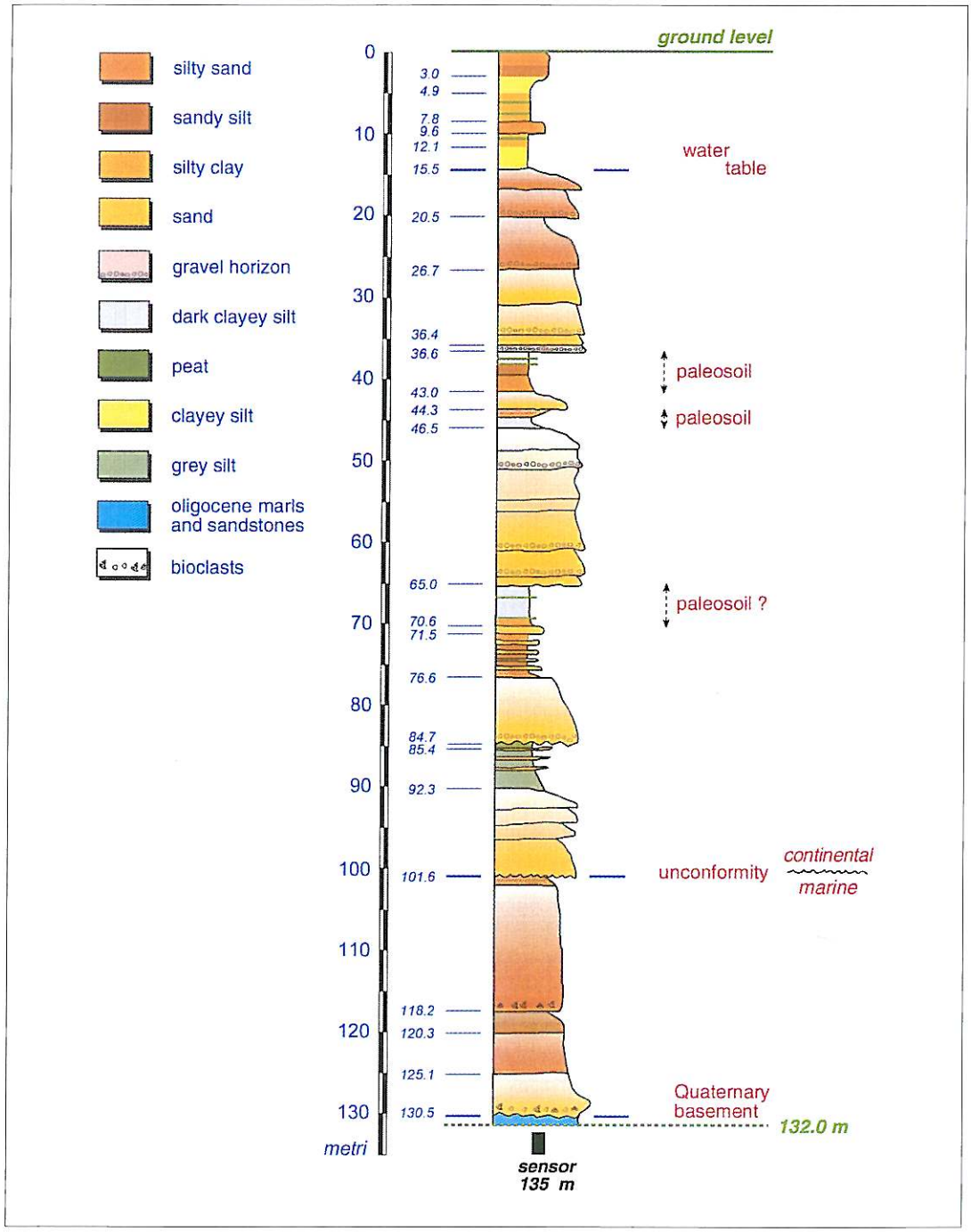

Fig. 2. Stratigraphic log of the borehole site.

ing the site response (Archuleta and Steidl, 1998; Kato *et al.*, 1998).

Figure 1a,b shows the studied area, the location of the borehole site (indicated by the asterisk in the map), the alluvial deposits outcropping in the area and the position of several exploratory wells (dots in the map) made by the Italian petroleum company (AGIP). It also shows the positions of the stations (a linear array) deployed during the seismic exploration experiment performed to constrain *P*- and *S*-wave velocity in the shallow alluvial layers (Malagnini *et al.*, 1997). Figure 1b also shows a cross-section that is part of a nearly NS seismic profile passing very close to the borehole site (see the position of the *Ferrara 1* well in the map and in the cross-section).

We selected this site because of the presence of a structural high (see section in fig. 1b) that reduces the depth of the quaternary deposits to a few hundreds of meters. This is the only place in the central part of the Po plain where a nearly 140 m deep well can reach the base of the quaternary alluvium, which in other places can be up to a few kilometers deep.

2. Site stratigraphy

The stratigraphy of the site was reconstructed during perforation of the well. Figure 2 shows the stratigraphic log of the first 130 m above the sensor. The most important feature is the base of quaternary alluvium located at a depth of 130 m, thus above the sensor installed at a depth of nearly 135 m, which guarantees that the broadband seismometer lies below the shallow alluvial layers. At a depth of nearly 100 m we found a continental-marine transgression, while the water table lies closer to the surface at nearly 15 m. These are the three most important discontinuities observed in the stratigraphic log shown in fig. 2. There are other minor horizons between 15 and 100 m named paleosoil in this figure. We expect that these horizons are less important for the goal of this study since they do not coincide with evident lithologic and geotechnical contrasts between the upper and lower layers. Moreover, these observations confirm the expectation about the shallowness of the quaternary basement, that we can consider as underlying bedrock for this area.

The geological structure of the site resulting from the stratigraphic log will help to constrain the depth of the layers where we need to measure anaelastic attenuation parameters and seismic velocities. We performed several experiments to estimate body wave velocities of the shallow alluvial layers that we present in the next section.

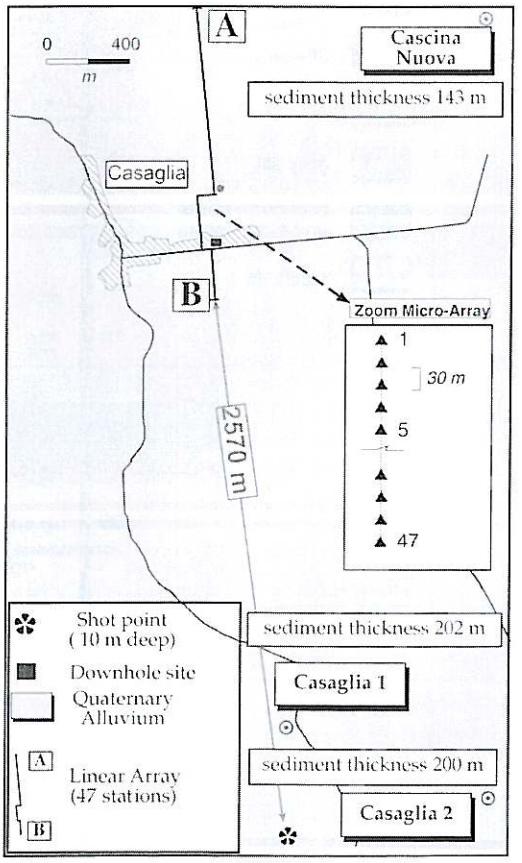

Fig. 3. Map of the area where the seismic exploration experiment took place: 47 seismic stations were deployed along the profile A-B. The solid rectangle shows the location of the borehole site near the Casaglia Village. The shot point was 2570 m from the first station of the array. The sediment thickness at the three closest wells is also indicated.

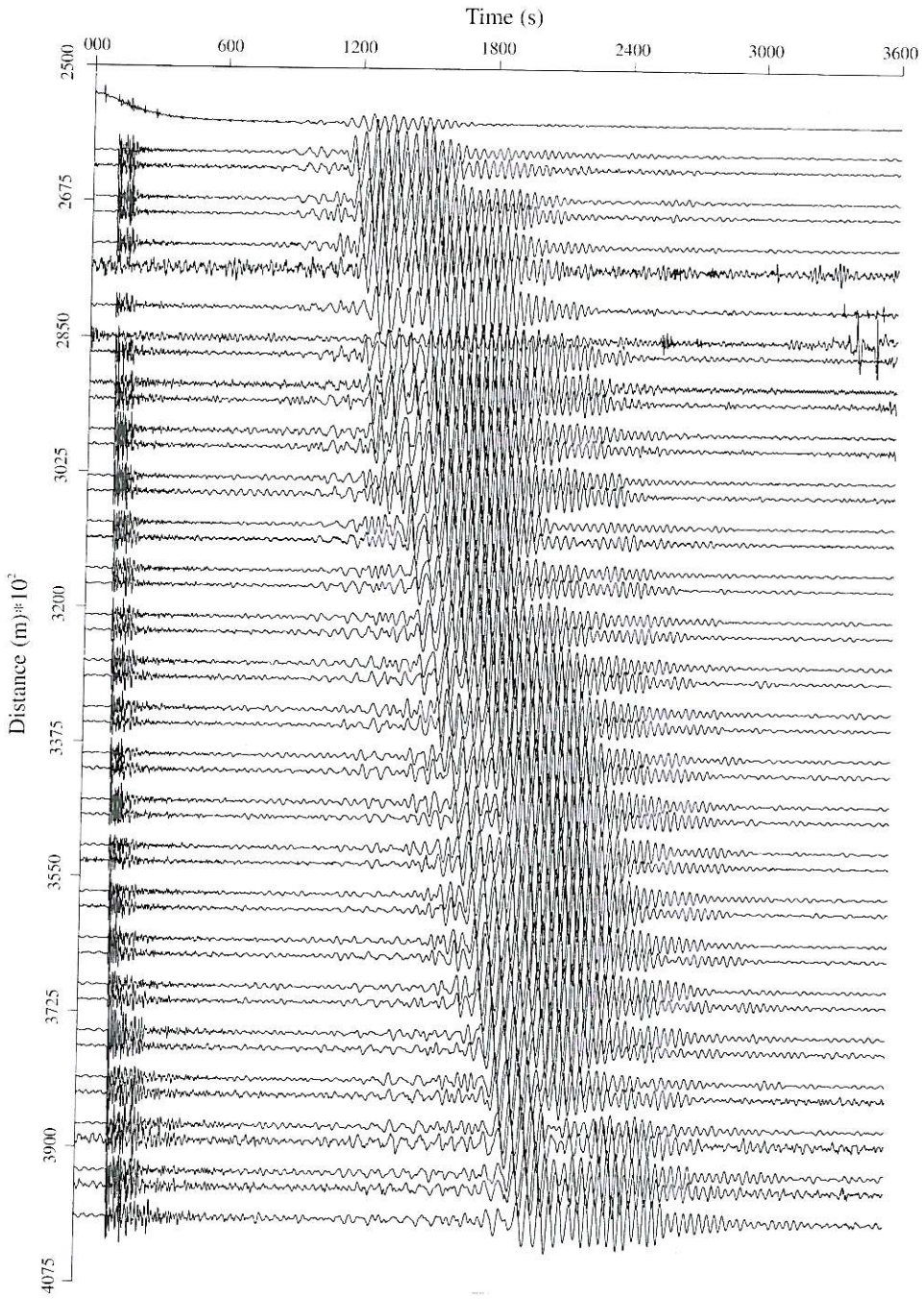

Fig. 4. Vertical component of ground-velocity time histories recorded along the array during the seismic exploration experiment (redrawn after Malagnini *et al.*, 1997).

3. Near-surface velocity model and attenuation

We performed a seismic exploration experiment to estimate the body wave velocities and the surface wave dispersion in the shallow layers. Figure 3 shows a map of the area where the experiment took place: 47 seismic stations were deployed along the profile A-B. The location of the borehole site close to the Casaglia Village is shown. The shot point was 2570 m from the first station of the array. Figure 4 shows the ground-velocity time histories (vertical components) recorded along the array during this experiment. We have indicated in fig. 3 the thickness of the alluvial sediments resulting from the stratigraphic log at the three closest AGIP wells. The positions of these wells help the comparison between the maps included in figs. 1a,b and 3. Malagnini *et al.* (1997) inverted the ground motion time histories shown in fig. 4 to estimate the body wave velocities of the shallow layers. They analyzed phase and group velocity dispersion of Rayleigh waves. Because of the methodology applied, their shear wave velocities are better constrained than *P*-wave velocities. The resulting velocity values are plotted in fig. 5.

We also performed cross-hole and up-hole measurements to constrain the body wave velocity in the first 80 m (Nardi *et al.*, 1996; Malagnini *et al.*, 1997). The resulting values are also shown in fig. 5. The comparison between the cross-hole, up-hole measurements and the values found by Malagnini *et al.* (1997) is very good for the *S*-waves down to a depth of 80 m.

According to these results and the stratigraphy, we use in the site response study a velocity model (see table I) for *S*-waves which is shown

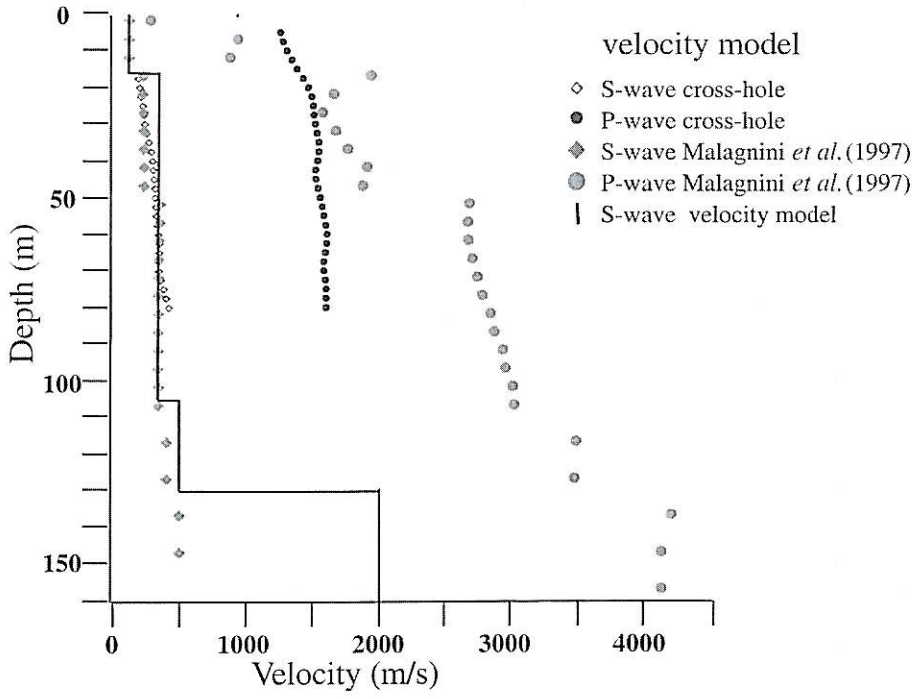

Fig. 5. Comparison between the *S*-wave velocity model used in this study (solid line and listed in table I) and the cross-hole up-hole measurements as well as the velocity model proposed for this area by Malagnini *et al.* (1997). The *P* wave velocity model is also shown for sake of comparison. The *S*-wave velocity model here adopted has been constrained by these experimental investigations.

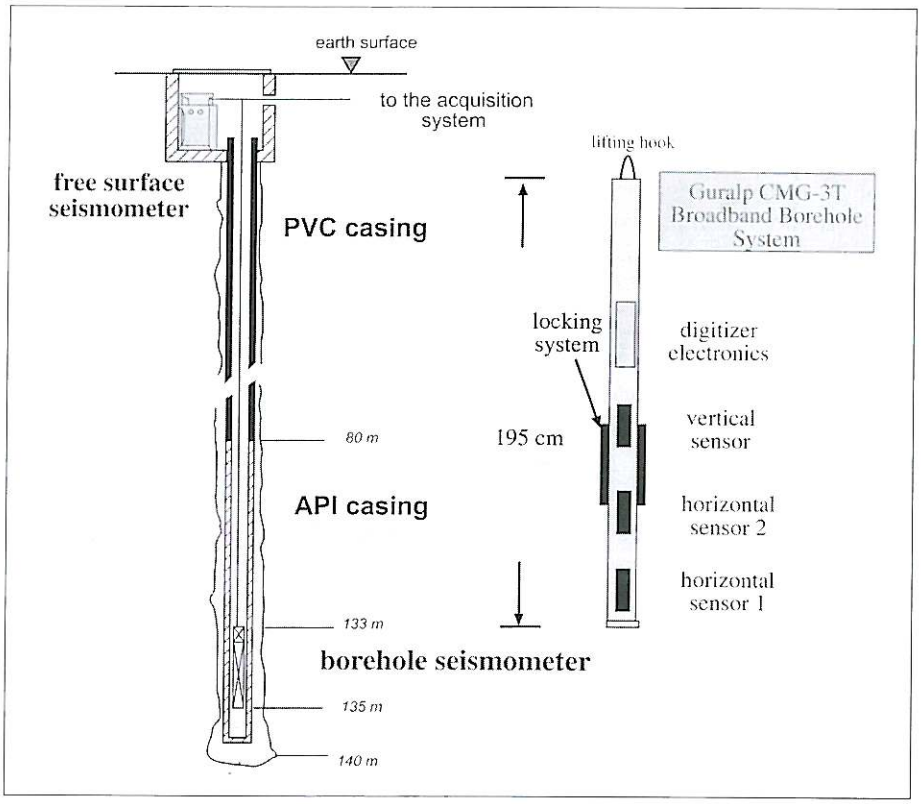

Fig. 6. Sketch showing the broadband sensor and its borehole installation.

Table I. *S*-wave velocity model.

Depth (m)	*S*-wave velocity (m/s)
0-15	140
15-103	300
103-130	490
Halfspace	2000

in fig. 5 with solid lines. The layer thickness agrees with the main discontinuities resulting from the analysis of stratigraphy (see the discontinuities at 15 m, 103 m and 130 m). The *S*-wave velocity value for the basement (below 130 m) is assumed according to the stratigraphy.

4. Installation and sensor characteristics

We installed a borehole weak motion broadband seismometer (Guralp CMG3T) because we were interested to record either local earthquakes or regional and teleseismic events. The high dynamic range seismometer was installed at a depth of 135 m, as shown in fig. 6. This figure also depicts a sketch of the well and the Guralp broadband borehole system. Figure 7 shows the sensor characteristics and the available dynamic range of the installed sensors compared to the Earth noise model (Agnew and Berger, 1978). The sensor has more than 140 db of dynamic range: at 1 Hz the clipping level is 0.01 g and there are almost 8 decades of dynamic range. We installed a second CMG3T at the

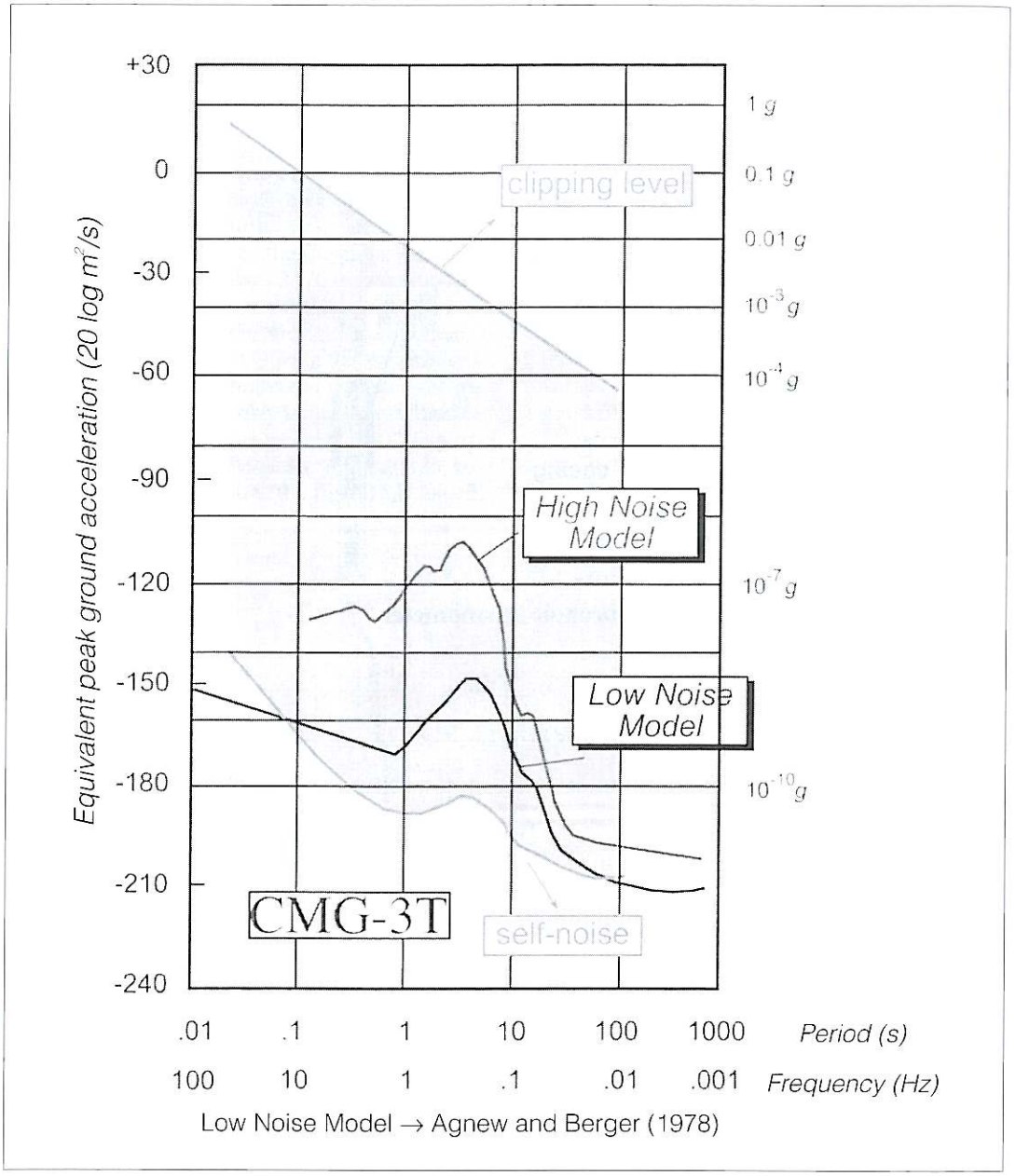

Fig. 7. Available dynamic range of the Guralp CMG3T installed in the borehole and at the surface compared with the low noise Earth model (Agnew and Berger, 1978).

Earth surface to compare the noise level and to determine the orientation of the borehole sensor.

The digital data are continuously recorded on a PC hard disk, which controls the sensor, data flow, mass centering and internal temperature. The expected data flow for the borehole and the surface sensors, with 24 bit resolution and 100 Hz sampling rate, is 1.4 Gbyte/week. The acquisition system requires large direct access storage and frequent backups on removable disks. We are modifying the acquisition system to transfer the data via digital line to the ING in Rome.

The installation of a sensor in a deep borehole does not permit its orientation, so that they have to be inferred indirectly. We use different methods to determine the orientation of the borehole seismometer. As a first step, we apply a cross-correlation analysis to a window of 200 s of teleseismic surface waves, recorded by the sensors at the surface and at depth (see fig. 8). Then we rotate the borehole horizontal components at steps of one degree and calculate the cross-correlation between borehole components and surface horizontal recordings, NS and EW oriented. Repeating this procedure the highest value of cross-correlation is found for a clockwise rotation of N116°. Borehole components rotated by N116° (see bottom traces in fig. 8) reproduce almost exactly the seismograms recorded at the surface as shown in fig. 8.

To check the correctness of this approach, we compared particle motions of the *P*-wave arrival for a local earthquake recorded both at surface and depth (see fig. 9). The first second of *P*-waves is quite coherent between the two sensors and the two particle motions become very similar after a clockwise rotation of N116°. Figure 9 shows the comparison between the surface and the borehole time histories after rotation, confirming the correctness of the orientation for the borehole horizontal components. As a final check, we compare the event back-azimuth resulting from a M_w = 5.4 earthquake located near Reggio Emilia at a distance of nearly 80 km from the borehole site. Figure 10 shows the borehole seismograms, the *P* waves on the rotated components and their particle motion. The event back-azimuth resulting from the event location procedure agrees reasonably well with the particle motion elongation.

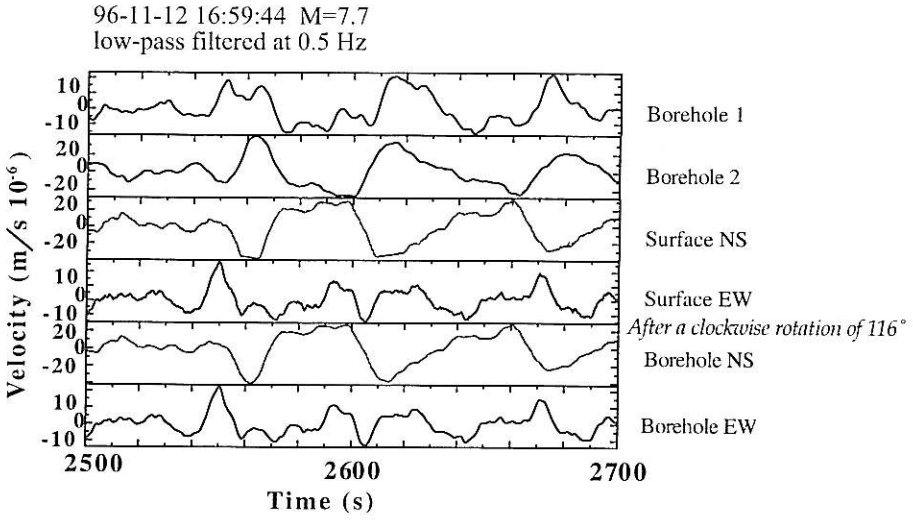

Fig. 8. Determination of the borehole sensor orientation using the horizontal recordings of a teleseismic event recorded both by the surface and the bottom sensors. The low-pass filtered waveforms recorded by the bottom sensor fit very well with those recorded at the surface after a clockwise rotation of 116°.

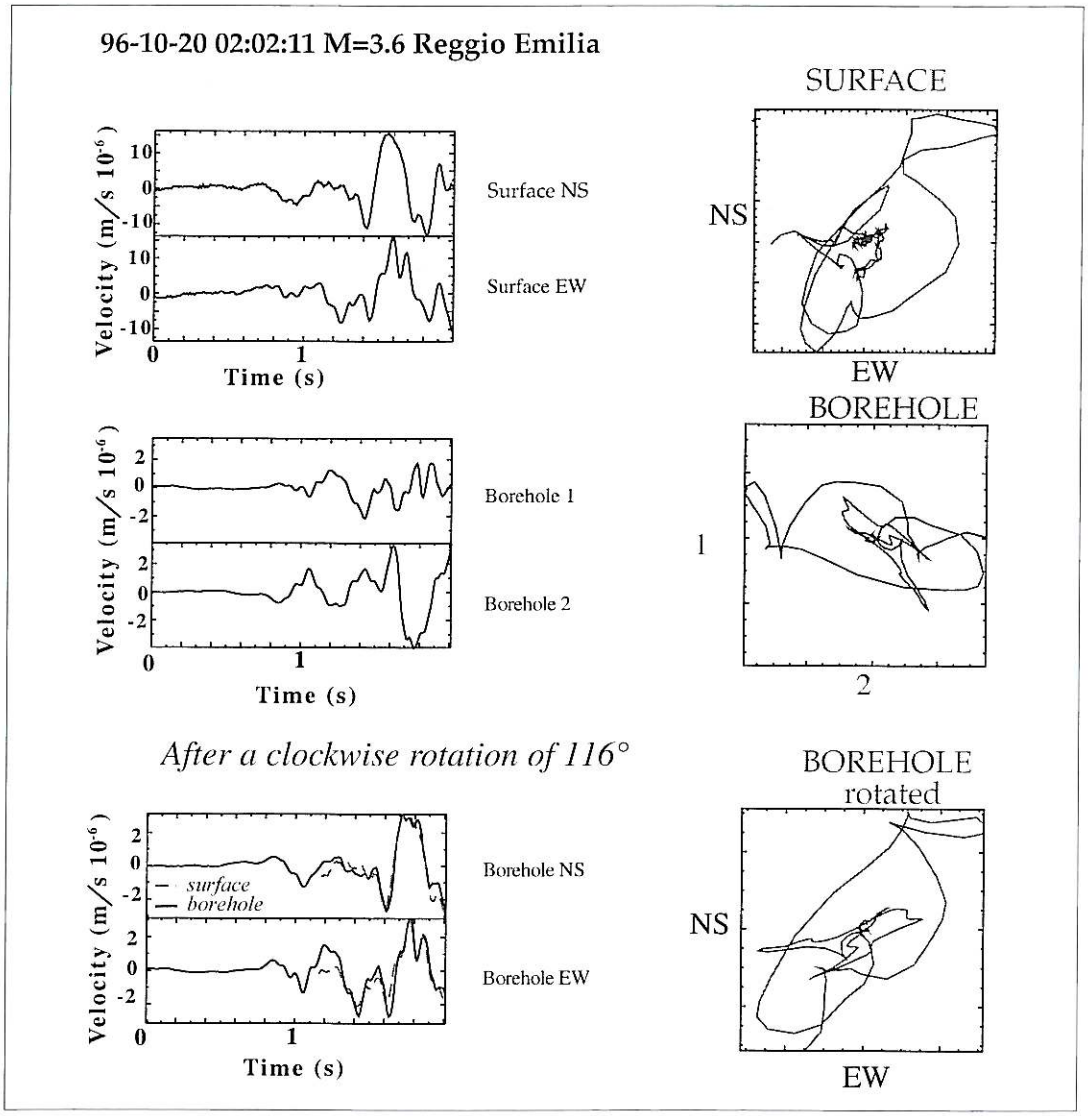

Fig. 9. Verification of the borehole sensor orientation using the particle motion analysis of the waveforms of a local earthquake recorded both by the bottom and surface broadband sensor.

All these analyses confirm the correct orientation of the borehole seismometer and emphasize the quality of the digital data recorded at this site. The waveforms recorded at this site were analyzed to verify the broadband sensor response and to characterize the site response of the shallow alluvial layers.

5. Ambient noise analysis

The installation of the borehole sensor guarantees a significant background noise reduction in an area where the anthropic noise is very high especially during the day. Figure 11 shows the Power Spectral Density (PSD) of ambient noise re-

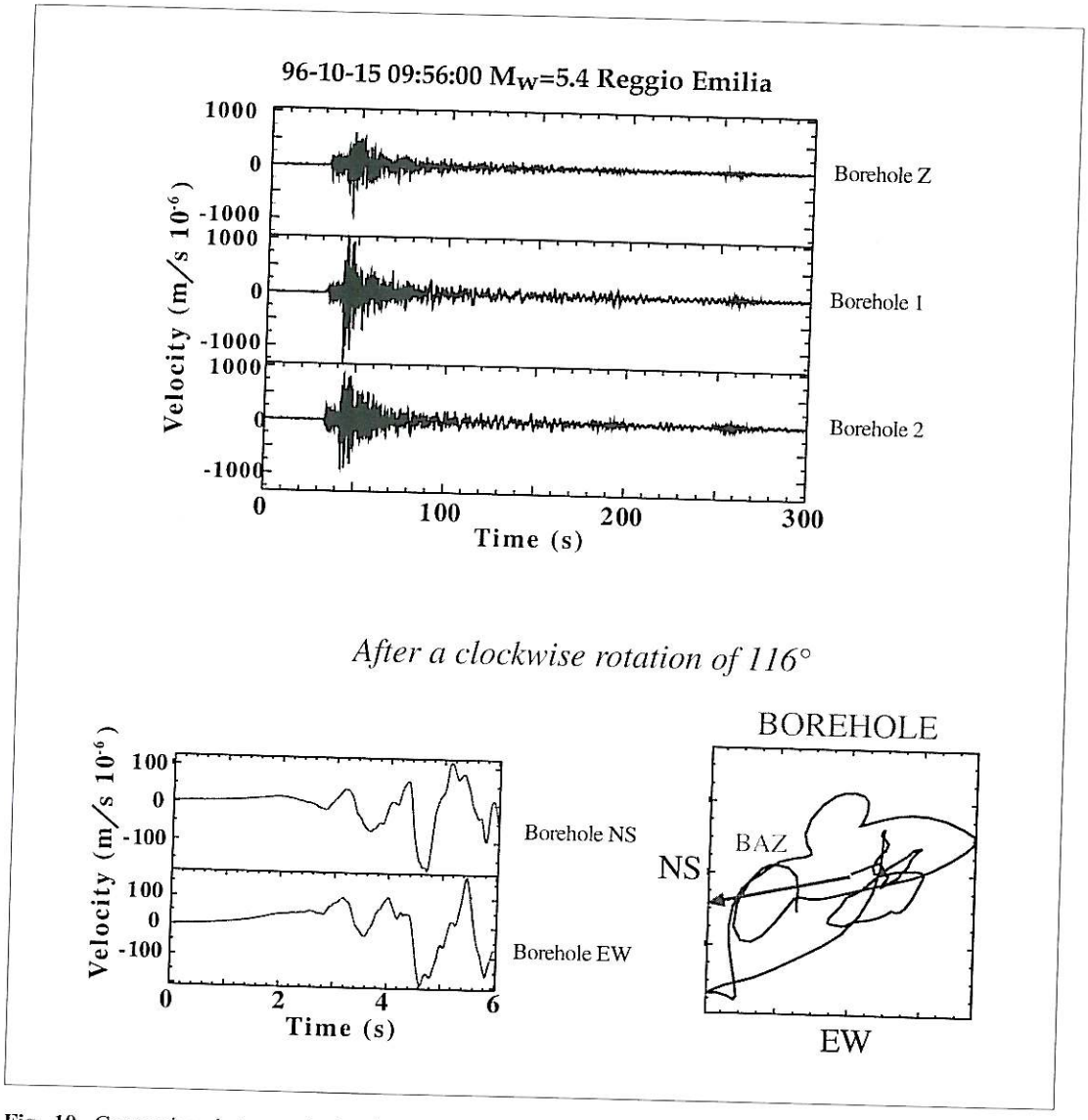

Fig. 10. Comparison between the borehole sensor orientation previously determined (see figs. 8 and 9) and the event back-azimuth of a *M* 4.8 earthquake located near Reggio Emilia and recorded at the borehole site.

sulting from the borehole and the surface sensors and compares them with the low noise model. The noise reduction for the borehole sensor is 2 decades in PSD at frequencies larger than 1.0 Hz. The reduction is even larger during the day, when the anthropic noise yields Power Spectral Density amplitudes much larger than those plotted in fig. 11.

The noise reduction is also evident looking at the vertical component of recordings of a teleseismic event recorded by the surface and the borehole sensors (see fig. 12). Before filtering, the surface seismogram is completely hidden by the noise and the event would not have been detected, while the seismic trace from the

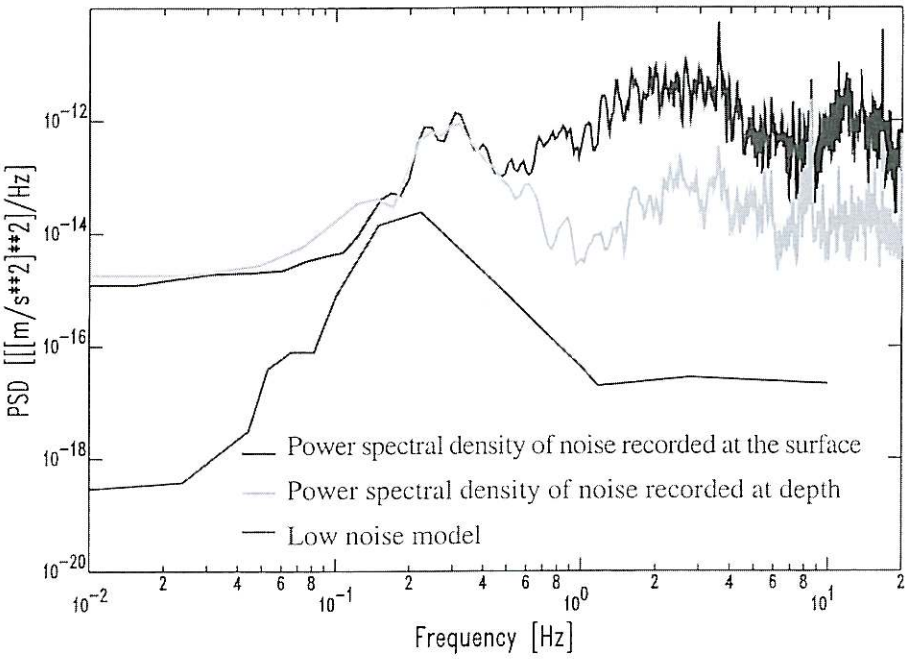

Fig. 11. Power Spectral Density (PSD) of ground noise recorded at the surface and at the bottom by the borehole sensor and comparison with the low noise model of Agnew and Berger (1978). This figure shows the noise reduction available for the borehole recordings.

borehole instrument is much clearer. Low pass filtering at 0.5 Hz yields identical seismograms, as expected considering that *S*-waves with a period of 2 s correspond to a wavelength of about 600 m.

The spectral ratio technique is commonly used to study the site effects. In this paper we applied this analysis to the ground noise recordings as well as to the local seismic events. 24 noise time windows of 40 s each were selected starting at the beginning of each hour (*e.g.*, 1st window from 00:00:00 to 00:00:40 a.m.). We compute the smoothed amplitude Fourier spectra for each time window for the surface and the borehole recordings. Spectral ratios of horizontal to vertical components (H/V, Nakamura, 1989; Lachet and Bard, 1994) were evaluated both at surface and at depth. The Hs/Vs spectral ratios at surface enhance a main peak at about 0.8 Hz with an amplification factor of 8 (fig. 13); borehole Hb/Vb ratio shows several small peaks, mainly at frequencies larger than 2 Hz, with a maximum amplification factor of 4 (fig. 13). Therefore, Nakamura's assumption that the ratio Hb/Vb provides unitary values is not completely fulfilled at our borehole site over the whole frequency bandwidth, although it is quite well satisfied in the frequency band 0.7-2 Hz. We also evaluated the double ratio Hs/Vs * Vb/Hb (Nakamura, 1989), which shows two amplification peaks at 0.8 Hz and at around 2 Hz; we will discuss these results in greater detail in the following.

6. Analysis of recorded seismograms

The availability of ground motion waveforms recorded simultaneously at the surface and at the borehole sensors is an ideal situation to estimate the response of the alluvial layers above the borehole sensor. Here we present some re-

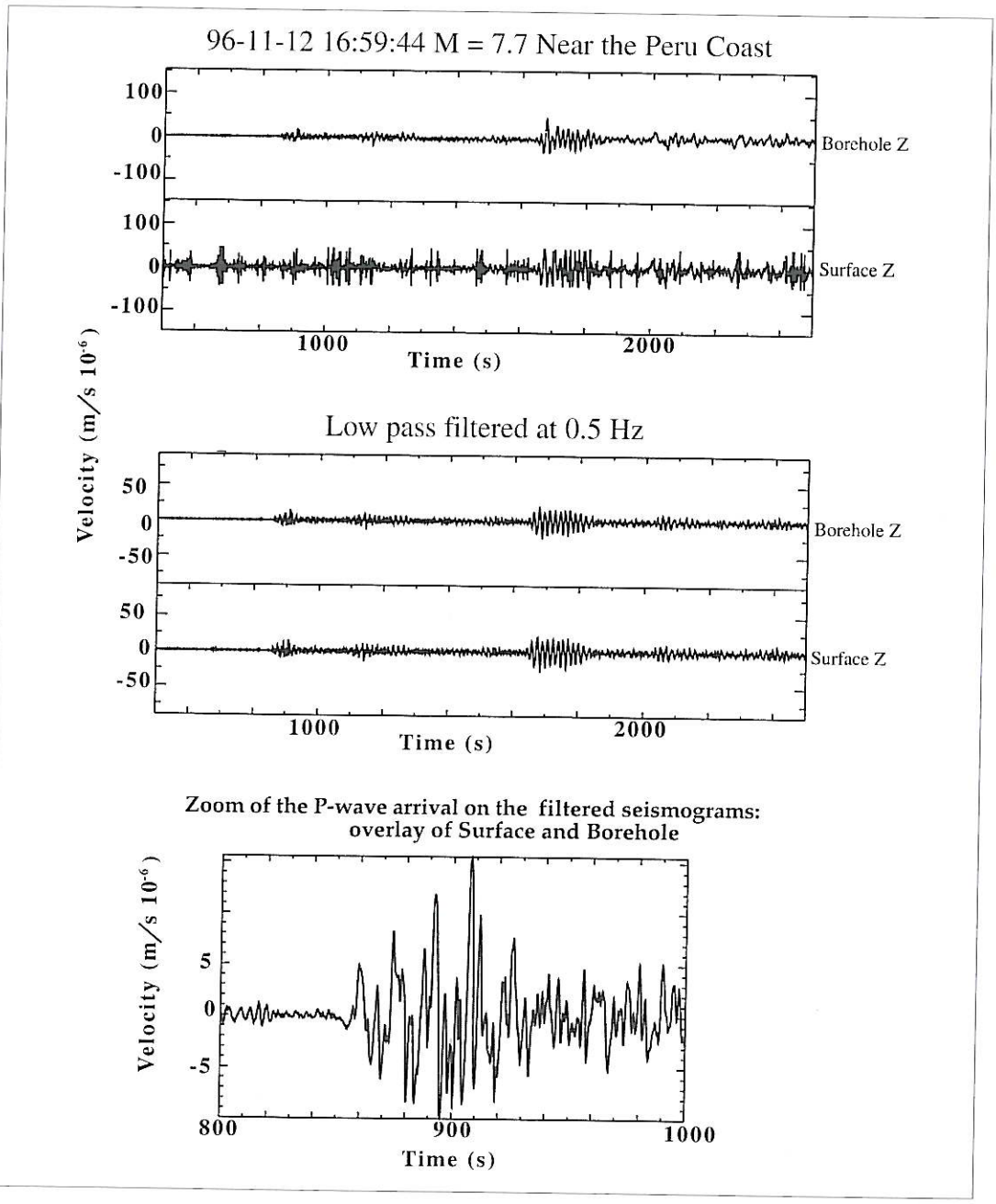

Fig. 12. Comparison between the surface and borehole recordings of a teleseismic event occurred near the coast of Peru: the upper traces show the unfiltered signals, while the bottom ones show the waveforms low-pass filtered at 0.5 Hz. The bottom panel points out the excellent agreement between the low-pass filtered waveforms recorded by the surface and borehole sensors.

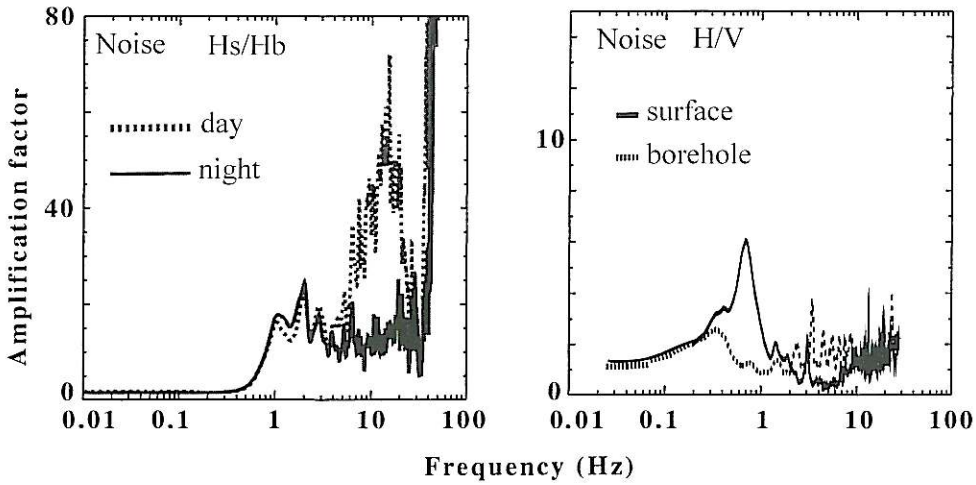

Fig. 13. Spectral ratios of ground noise: the left panel shows the spectral ratio between the horizontal components recorded by the surface and the borehole sensors: the dotted and solid lines show the average spectral ratios computed using signal's time windows recorded during the day and the night, respectively. The right panel shows the horizontal to vertical spectral ratios (Nakamura, 1989) resulting from the surface and the borehole recordings.

sults of a site effect investigation performed by applying the spectral ratio technique to the recordings of local seismic events.

A seismic sequence started in the Reggio Emilia region (Northern Italy) on October 15 (at 09:56 GMT) with a M_w 5.4 earthquake located about 80 km far from the recording site (see the map in fig. 14). We recorded the mainshock and several aftershocks at the Ferrara site both with the surface and borehole sensors. We selected the 8 best recorded seismic events in the magnitude range between 2.2 and 3.6. We computed smoothed amplitude spectra from horizontal components of ground motion selecting a time window spanning the whole seismogram including *P*, *S* and coda phases and ending at a 40 s lapse time. In fig. 14 we show the spectral ratios for each of the seismic events analyzed in this study.

The use of borehole recordings (considered as bedrock ground motions) to compute spectral ratios requires correction for the destructive interference caused by the downgoing wave field (reflected by the free surface). For this reason, we corrected the surface recordings by multiplying for the normalized coherence $[C^2(f)]$ between the surface and borehole wave-fields defined as follows (see fig. 14)

$$C^2(f) = |S_{12}(f)|^2 / S_{11}(f) S_{22}(f) \qquad (6.1)$$

where $S_{11}(f)$ and $S_{22}(f)$ are Fourier transforms of the auto-correlations and $S_{12}(f)$ is the Fourier transform of the cross-correlation (Steidl *et al.*, 1996). We compare in fig. 14 the uncorrected spectral ratio of one event with that multiplied by the coherence function: this correction reduces the amplitudes of the first peak at 0.6-0.7 Hz. We apply this correction to the spectral ratios of surface to borehole horizontal components of recorded ground motions and also evaluate their log-normal average corrected for coherence (fig. 15).

We computed the H/V (Nakamura, 1989) ratios for all the earthquake recordings and we calculated the average ratio as a function of frequency. At the surface we find a general amplification of a factor 2.5 in the frequency band between 0.3 and 3 Hz, with no well defined peaks; at the borehole, the H/V shows several peaks with low (less than 2.0) amplification

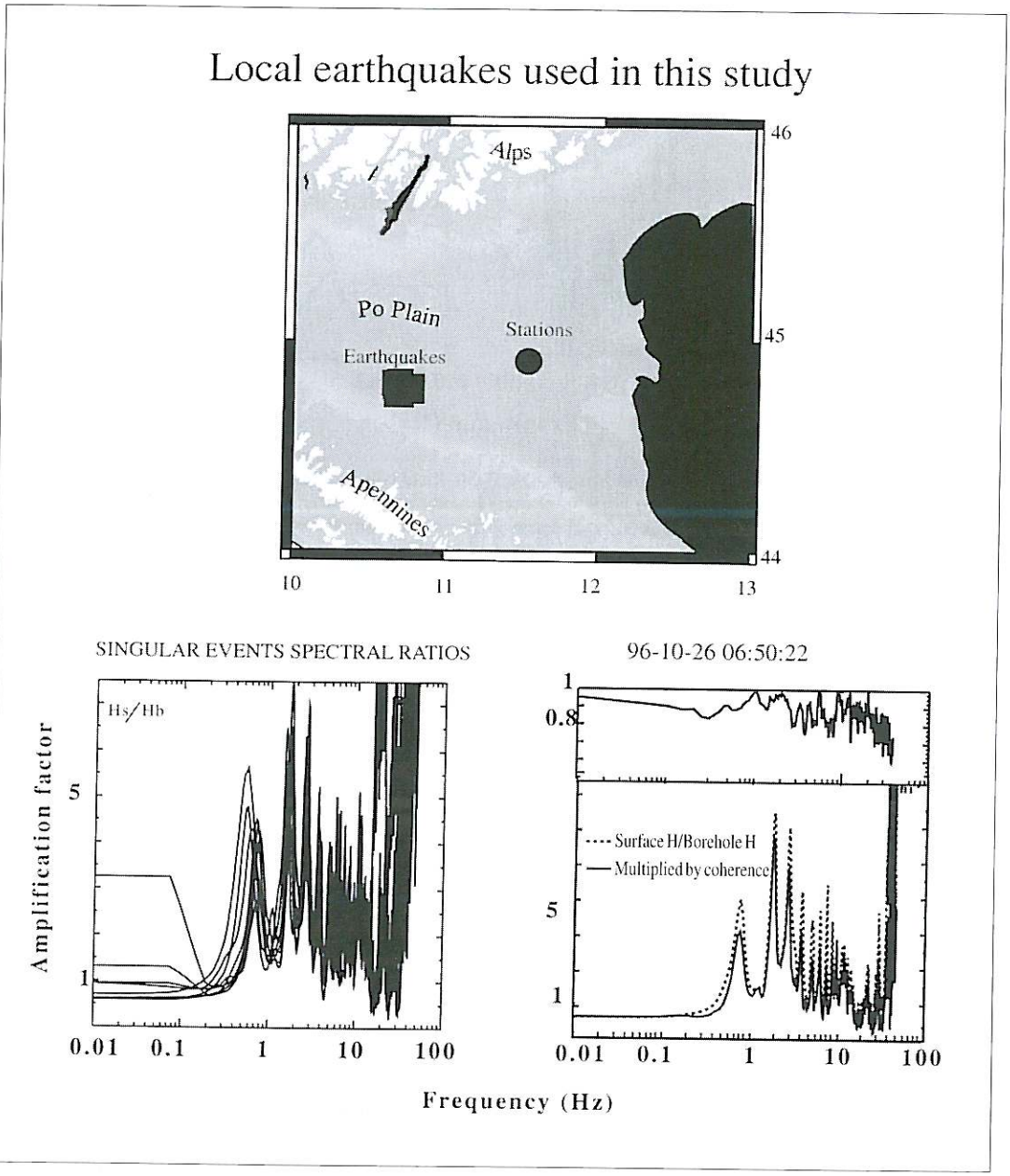

Fig. 14. Spectral ratio analysis of local earthquake recordings: the seismic events here analyzed belong to the seismic sequence that struck the Reggio Emilia area on October 1996 (see the map in the upper panel). The spectral ratio for each selected earthquake is shown in the bottom left panel. The bottom right panel shows the coherence function (C^2) computed from the surface and borehole wave-fields for one of the events. We compare in this panel the uncorrected spectral ratio for the selected earthquake and that after correction for the coherence as a function of frequency.

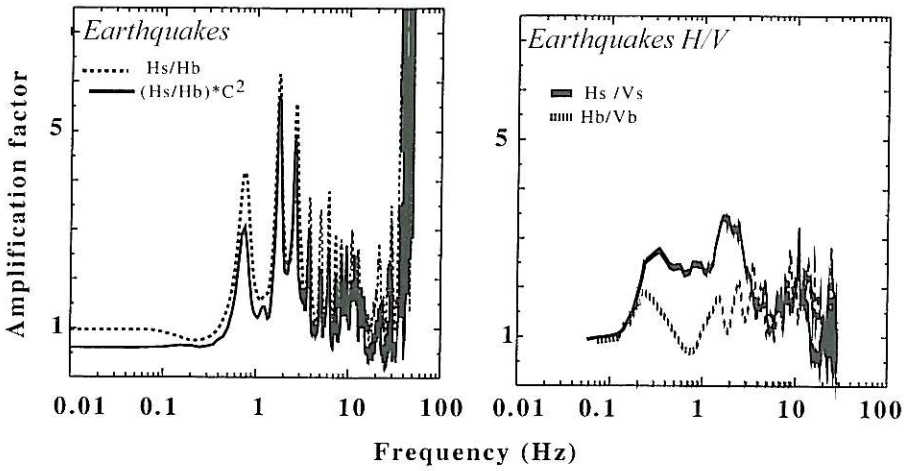

Fig. 15. Average spectral ratios computed from the available local earthquake recordings. Left panel shows the average spectral ratio resulting from the horizontal components of surface and borehole recordings. The right panel show the horizontal to vertical average spectral ratio (Nakamura, 1989) computed from the waveforms recorded by the surface (solid line) and the borehole sensor (dashed line).

factor (see fig. 15). Among the different techniques used, the H/V ratio is the only one that does not identify the fundamental resonant peak at this site. It is interesting to note that the double ratio ((Hs/Vs)*(Vb/Hb); see fig. 16) computed on the event recordings enhances hints of the first two peaks of amplification at about 0.6 Hz and 2 Hz, which were not visible in the single Hs/Vs ratio. This suggests that the borehole recording is probably not completely free from the influence of the local geology above it.

In order to interpret better the spectral ratios computed both on ambient noise and earthquake recordings it is useful, when geotechnical information is available, to compare the empirical site response estimates with a theoretical calculation. We computed the horizontal theoretical response of the shallow layers by means of the Haskell and Thomson method (Haskell, 1953; Thompson, 1950). The computation is done for a *SH* vertically incident waves using the velocity model in fig. 5 and the Q value reported in table II (Malagnini *et al.*, 1997).

The theoretical site response is shown in fig. 16 (heavy solid line) where it is compared with the different estimates obtained empirically. It compares reasonably well with the average estimate resulting from earthquake recordings (black thin curve) which is lower than the model. The amplification peaks at 0.8, 2 and 3 Hz are consistent.

The 0.8 Hz peak is lower by a factor 5/3 with respect to the theoretical transfer function. The Nakamura spectral ratio shows only the fundamental peak at about 0.8 Hz consistently with the model. Surface to borehole noise spectral ratio has amplification values several times higher than the theoretical transfer function but still the first three peaks at lower frequencies (1, 2, 3 Hz) are close to the resonance frequencies found in the theoretical modeling.

7. Conclusive remarks

We present here the results of a project focused on the study of local site effects using the recordings of a borehole broadband seismometer located in the alluvial basin of the Po River (Po plain). This study represents the first investigation in this area made with high quality digital data. For this reason, attention was given

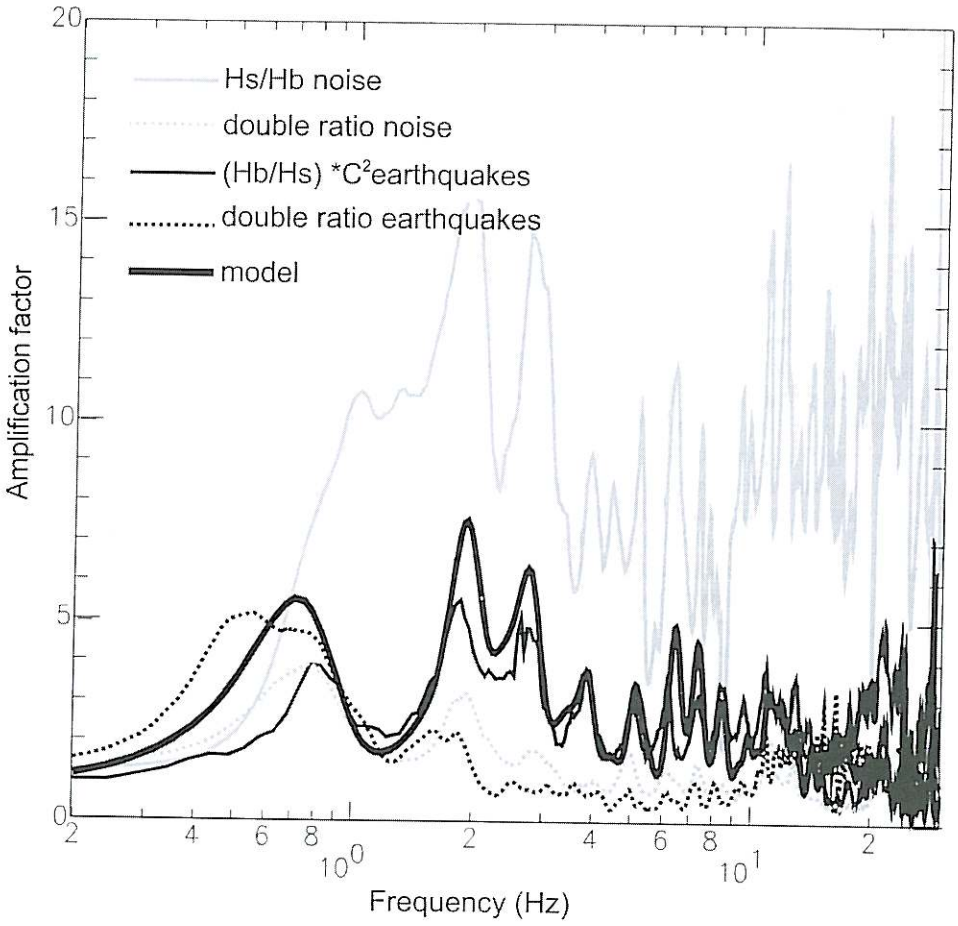

Fig. 16. Spectral ratios computed from noise time windows as well as from the horizontal recordings of local earthquakes recorded by the surface and the borehole sensor compared to the theoretical transfer function obtained by the Haskell-Thomson method. For both ground noise and local earthquake recordings we have plotted the spectral ratio resulting from the horizontal components at the surface and at the borehole; the average spectral ratio resulting from earthquake recordings is corrected for the coherence function. We also show the double ratio for both background noise and earthquakes, which consists on the ratio between the horizontal to vertical components (H/V) spectral ratio at the surface and at the borehole. The theoretical function has been computed using the velocity model shown in fig. 5 and listed in table I and assuming a *S*-wave velocity of 2.0 km/s at 1 km of depth.

Table II. Adopted anelastic parameters.

Depth (m)	*Qp*	*Qs*
0-50	20	20
50-140	50	50

to the data processing and the control of the recorded data quality. The estimated noise reduction is encouraging and emphasizes the importance of such a project. The anelastic attenuation properties are taken from previous studies (Malagnini *et al.*, 1997). We collected observa-

tions to constrain the body wave velocity of the shallower alluvial layers overlying the borehole sensor. The analysis of the stratigraphy and of seismic data, recorded during an exploration experiment as well as by cross-hole and up-hole measurements, constrains the body wave velocity in the first 150 m, from the Earth surface to the quaternary basement. The resulting velocity model agrees well with the stratigraphy.

We analyzed spectral ratios of noise time windows as well as local earthquakes located 80 km away from the borehole site. We compared these spectral ratios with the prediction of a theoretical model based on the Haskell-Thomson approach. The results obtained in this study can be summarized as follows:

– Surface on borehole noise spectral ratios show a sharp increase at about 0.7 Hz and three peaks at about 1 Hz, 2 Hz and 3 Hz. The amplification values for these peaks reach a factor of 20. Above 4 Hz, the day and night averages differ substantially, the day spectral ratio being very high due to anthropic noise (up to 70) (see fig. 13).

– Nakamura noise spectral ratios enhance a main peak at about 0.8 Hz with an amplification factor of 8; no large differences are observed in the day and night averages (fig. 13).

– Surface over borehole seismic events spectral ratios are reasonably stable for the different events (all the earthquakes come from the same azimuth). The amplitude of the first peak (0.8 Hz) varies more than the others in a range between 3 and 6. The average spectral ratio shows an amplification factor of about 3 at 0.6 Hz and of about 6 between 2 and 3 Hz, that are the highest resonant peaks (see fig. 16). Assuming an average shear-wave velocity of 400 m/s, the low frequency peak at 0.8 Hz is consistent with the resonance of a 125 m thick layer that coincides with the thickness of the alluvium for this site.

Acknowledgements

We wish to thank Emilia Romagna Region for its support in this project and in drilling the wells. We appreciated the useful and valuable collaboration of Gilberto Goberti during the installations of the sensor and the data acquisition. The support of the Ferrara Municipality was crucial to complete the project. We also thank R. Console, A. Basili and E. Boschi for encouraging this research and for useful conversations.

REFERENCES

AGNEW, D.C. and J. BERGER (1978): Vertical seismic noise at very low frequency, *J. Geophys. Res.*, **83**, 5420-5424.

ARCHULETA, R.J. and H.J. STEIDL (1998): ESG studies in the United States: results from borehole arrays, in *Proceedings of the Second International Symposium on the Effects of Surface Geology on Seismic Motion, Yokoama, Japan, 1-3 December 1998*, vol. 1, 3-14.

HASKELL, N.A. (1953): The dispersion of surface waves in multi-layered media, *Bull. Seismol. Soc. Am*, **43**, 27-34.

KATO, K., M. TAKEMURA, T. KONNO, S. UCHIYAMA, S. IIZUKA and R.L. NIGBOR (1998): Borego Valley downhole array in Southern California: instrumentation and preliminary site effect study, in *Proceedings of the Second International Symposium on the Effects of Surface Geology on Seismic Motion, Yokoama, Japan, 1-3 December 1998, Balkema*, vol. 1, 209-217

LACHET, C. and P.Y. BARD (1994): Numerical and theoretical investigations on the possibilities and limitation of Nakamura's technique, *J. Phys. Earth*, **42**, 377-397.

MALAGNINI, L., R.B. HERMAN, A. MERCURI, S. OPICE, G. BIELLA and R. DE FRANCO (1997): Shear-wave velocity structure of sediments from the inversion of explosion-induced rayleigh waves: comparison with cross hole measurements, *Bull. Seismol. Soc. Am*, **87**, 1413-1421.

NAKAMURA, Y. (1989): A method for dynamic characteristics estimation of surface using microtremor on the ground surface, *Q. Rep. Railw. Tech. Res. Inst., Tokyo* , **30**, 1.

NARDI, A., F. ARDIZZONI, R.M. AZZARA, M. COCCO, L. DALL'OLIO, A. DELLADIO, G. GOBERTI and L. MALAGNINI (1996): Progetto downhole in pianura Padana, *Publication of the Istituto Nazionale di Geofisica, Roma*, No. 575 (in Italian).

STEIDL, H.J., A.G. TUMARKIN and R.J. ARCHULETA (1996): What is a reference site?, *Bull. Seismol. Soc. Am*, **86**, 1733-1748.

THOMPSON, W.T. (1950): Transmission of elastic waves through a stratified solid medium, *J. Appl. Phys.*, **21**, 89-143.

(received October 25, 2000;
accepted February 10, 2001)